Alimentary tract as entry route for hantavirus infection

Running title: Gastrointestinal hantavirus transmission

Article type: Observation

Peter T. Witkowski[1*], Casey C. Perley[2], Rebecca L. Brocato[2], Jay W. Hooper[2], Christian Jürgensen[3], Jörg-Dieter Schulzke[4*], Detlev H. Krüger[1#], Roland Bücker[4#]

[1]Institute of Virology, Charité – Universitätsmedizin Berlin, Germany

[2]Virology Division, United States Army Medical Research Institute of Infectious Diseases (USAMRIID), Ft. Detrick, Maryland, USA

[3]Division of Hepatology and Gastroenterology, Charité – Universitätsmedizin Berlin, Germany

[4]Institute of Clinical Physiology, Charité – Universitätsmedizin Berlin, Germany

[*]Corresponding authors:
Peter T. Witkowski, Institute of Virology, Helmut-Ruska-Haus, Charité – Universitätsmedizin Berlin, Charitéplatz 1, 10117 Berlin, Germany
Tel: +49 30 450 525 089, Email: Peter.Witkowski@charite.de
and
Jörg-Dieter Schulzke, Dept. of Gastroenterology, Infectiology and Rheumatology, Division of Nutritional Medicine / Institute of Clinical Physiology, Charité – Universitätsmedizin Berlin, Hindenburgdamm 30, 12203 Berlin, Germany
Phone +49 30 450 514 531, Email: joerg.schulzke@charite.de

[#] shared senior authorship

ABSTRACT

Hantaviruses are zoonotic agents that cause hemorrhagic fever with renal and/or cardiopulmonary manifestations, reaching fatality rates of up to 50%. A large proportion of hantavirus patients also suffer from gastrointestinal complications of unclear cause. Puumala hantavirus (PUUV), the predominant endemic hantavirus in Europe, is associated with mild forms of hemorrhagic fever with renal syndrome. PUUV is transmitted to humans by exposure to aerosolized excrement from infected rodents. In this study we demonstrate that PUUV can also infect via the alimentary tract. PUUV retains infectivity in gastric juice for at least some time in pH >3 and is able to infect polarized human Caco-2 monolayers. This small intestinal cell model exhibited viral association with endosomal antigen EEA-1, followed by virus replication and loss of epithelial barrier function with concomitant basolateral (serosal) occurrence of viruses. Cellular disturbance and depletion of the tight junction protein ZO-1 appeared after prolonged hantavirus infection. Subsequent cell rounding and detachment was observed, leading to paracellular leakage. Moreover, experimental PUUV infection of Syrian hamsters by the intragastric route led to seroconversion and protection against challenge by lethal Andes virus in a dose-dependent manner, confirming that PUUV retains infectivity when administered directly to the gut. These data are the first report of PUUV infections via the alimentary tract and demonstrate the importance of this route of transmission for public health considerations.

Keywords

Hantavirus, Puumala virus, hemorrhagic fever with renal syndrome, zoonoses, virus entry, gastrointestinal infection, gastric barrier, epithelial barrier, tight junction, transmigration, endocytosis, hamster model

49 **Importance**

50 Hantaviruses are zoonotic pathogens, transmitted to humans by small animals, which cause
51 severe hemorrhagic fevers worldwide. To date these viruses are generally thought to be
52 transmitted by one of two routes: either through the inhalation of aerosolized virus from
53 infected animal droppings (the predominant route of infection) or by rodent bites. It had been
54 observed before that Andes hantavirus can infect hamsters by intragastric application, though
55 the route was less efficient than others tested and the mechanisms were not investigated. In
56 this study we show that PUUV, a hantavirus endemic to Europe, is capable of surviving in
57 gastric juice, crossing the gastric barrier and causing a productive infection in the Syrian
58 Hamster model of PUUV infection. We conclude that the alimentary tract is a productive path
59 of infection. Our findings provide new insight into the mechanisms of hantavirus infection
60 and have implications for hantavirus epidemiology and outbreak prevention measures.

61

INTRODUCTION

Hantaviruses are zoonotic viruses harbored by small mammals such as rodents, shrews, or bats. They can cause disease in humans, leading to hemorrhagic fevers of varied severity. Old World hantavirus infections usually lead to Hemorrhagic Fever with Renal Syndrome (HFRS), with case fatality rates of up to 15%, while the clinical course New World hantavirus infection is mainly linked with Hantavirus Cardiopulmonary Syndrome (HCPS), also known as hantavirus pulmonary syndrome, and case fatality rates of up to 50%. The symptomatology of both manifestations is not strict and mixed clinical courses, as well as asymptomatic infection, can occur (1).

In Europe most cases of hantavirus disease are caused by one of two strains of virus. Human infection with Puumala virus (PUUV), which is harbored by the bank vole (*Myodes glareolus*), typically leads to less severe disease, while individuals infected with Dobrava-Belgrade virus (DOBV), whose three genotypes *Dobrava*, *Kurkino*, and *Sochi* are carried by rodents of the genus *Apodemus*, are more likely to exhibit severe symptoms (1). Pathogenic hantaviruses are generally thought to enter the human body by inhalation of contaminated droppings from infected host animals, followed by infection of the lung epithelium. Moreover, in rare cases, rodent bites were reported to be the cause of infection (2).

Hantaviruses preferentially use different β-integrins and CD55/DAF for cell entry (3 - 5). However, the presence of some of the receptor molecules on the basolateral side of the affected tissues requires effective disruption, or at least penetration, of the cell barrier, as shown *in vitro* for different tissue types (6). Interference with cellular barrier function of infected tissues can lead to capillary leakage and is a crucial aspect of hantavirus pathogenesis (2). As a prototypical member of the genus *Hantavirus*, Hantaan virus, was shown to enter cells by clathrin-dependent endocytosis after receptor-mediated binding to the cell surface (7).

Besides the typical organ preference of hantavirus disease, several studies have shown that the majority of patients exhibits hemorrhagic gastropathy (8). Moreover, in the Syrian hamster model established for South American Andes virus (ANDV) intragastric inoculation can result in lethal disease, albeit with a higher 50% lethal dose (LD_{50}) than the more effective intramuscular, subcutaneous, intranasal, and intraperitoneal delivery routes (9). In rare cases, contact to contaminated food was named as a possible risk factor for human hantavirus infections (10). These findings demonstrate that the gut is affected in human hantavirus disease and that the infection via the alimentary tract is a possible route of transmission.

A gastrointestinal transmission route for HFRS-causing hantavirus has not been explicitly proposed or excluded for either humans or rodent infection. For this reason we conducted both *in vitro* and *in vivo* studies with PUUV, the main European hantavirus responsible for HFRS, to ascertain its viability as a route of infection. *In vitro* we investigated susceptibility of the human small intestinal epithelium for hantavirus infection, based on the polarized Caco-2 cell culture system, an established model for intestinal barrier function, and investigated the resistance of virus particles to gastric juice. *In vivo* we demonstrated that intragastric infection of Syrian hamsters with PUUV can lead to seroconversion and protective immunity against subsequent lethal hantavirus challenge.

MATERIALS AND METHODS

Cell culture

Caco-2 cells (ATCC HTB-37) were cultivated at 37°C with 5% CO_2 and maintained in minimal essential medium (MEM) with 10% fetal bovine serum, and 1% L-glutamine. For immunofluorescence assays (IFA) Caco-2 cells were grown on coverslips in 24-well plates. For measurement of transepithelial electrical resistance (TER) the cells were seeded on

permeable PCF filter inserts with an area of 0.6 cm^2 and a pore size of 0.4 µm (Millipore, Germany). The cells were grown for 21 days for differentiation to small intestinal properties. Cell medium was replaced every two or three days. Transepithelial electrical resistance (TER) was measured by an ohmmeter fitted with chopstick electrodes (EVOM, World Precision Instruments, USA) before infection and confluent cell monolayers showing epithelial resistance with above 500 $\Omega \cdot cm^2$ were used for experiments.

Virus cultivation

For *in vitro* studies: PUUV strain Sotkamo was grown on Vero-E6 cells (ATCC CRL-1586; American Type Culture Collection, Manassas, USA) under standard cell culture conditions. Viruses were harvested by ultracentrifugation through a sucrose cushion in order to remove residual cell culture components and titers were determined by focus titration, as previously described (11). For *in vivo* studies: PUUV strain K27 and ANDV strain Chile-9717869 were grown on Vero-E6 cells in T-150 flasks and collected from infected-monolayer supernatants. Cell debris were removed by low speed centrifugation (2,500 rpm in a table top centrifuge), and virus was twice plaque purified. Virus stocks were aliquoted and stored at -60ºC or colder (12).

Virus inactivation by gastric juice

Gastric juice was taken from adult patients who underwent gastroscopy for other diagnostic reasons and were not treated by any acid suppressing medication. According to the Declaration of Helsinki (Ethical Principles for Medical Research Involving Human Subjects) all patients gave written informed consent.

pH was measured and dilution series were performed by solution of NaOH pellets. PUUV stock was incubated with gastric juice of different pH for given time periods of 0 – 15

minutes. Subsequently pH was set to a value of 7 and culture medium was added. The treated virus solution was serially diluted ant titrated on Vero-E6 cells.

Cell infection experiments

Caco-2 cells on coverslips or filter inserts were infected for 1 h at a multiplicity of infection (MOI) of 0.1 - 1.0. Afterwards remaining inoculum was washed away and the cells were incubated in culture medium at described conditions. TER measurements in filter inserts were conducted every 24 h. Samples for microscopy were fixated with 4% methanol-free paraformaldehyde, afterwards blocked by 25 mM glycine in phosphate buffered saline (PBS). Samples for quantitative PCR (qPCR) were collected in AVL buffer (Qiagen, Germany) in case of culture medium or RLT buffer (Qiagen) in case of cells and stored at -80°C. For virus titration from infection kinetics culture medium was stored at -80°C.

Quantitative RT-PCR

RNA from culture supernatants and cell lysates was extracted according to manufacturer´s specifications by QIAamp Viral RNA Mini Kit and RNeasy Mini Kit, respectively. Reverse transcription was performed with M-MLV reverse transcriptase (Invitrogen, Germany). Virus quantification was conducted by real-time RT-PCR, as described before (13).

Fluorescence microscopy

Fluorescence staining and confocal laser-scanning microscopy (CLSM) was performed as previously described (14). The following antibodies were used: anti-ZO-1 (Zonula occludens protein-1), anti-EEA1 (early endosomal antigen 1), anti-hantaviral nucleocapsid protein (1:100), Alexa-Fluor488 goat anti-mouse or -rabbit IgG, and Alexa-Fluor594 goat anti-mouse or -rabbit IgG (1:500; Invitrogen). Cell nuclei were stained with 4’-6-diamidino-2-phenylindole dihydrochloride (DAPI, 1:1,000).

Epithelial apoptosis

Occurrence of apoptosis was visualized by TUNEL assay (terminal deoxynucleotidyl transferase–mediated deoxyuridine triphosphate nick-end labeling, In-situ Cell Death Detection Kit-Fluorescein, Roche, Germany) in Caco-2 monolayers four days post infection as previously described (14). Percent of apoptotic events were calculated as ratio of all cells in a low-power field (200 x magnification). Six pictures per sample containing more than 1,300 cells each were counted for the analysis.

Animal experiments

Female Syrian golden hamsters, age 6-8 weeks (Harlan, Indianapolis, USA) were anesthetized by inhalation of vaporized isoflurane using IMPAC 6 veterinary anesthesia machine. Once anesthetized hamsters were challenged intragastrically with 1,000 PFU PUUV, 10,000 PFU PUUV, or 10,000 PFU γ-irradiated PUUV ($3x10^6$ rad) diluted in 1mL sterile PBS delivered by a 3 mL syringe with a 2-inch 18 gauge gavage needle. Forty-two days post PUUV infection hamsters were challenged intramuscularly (i.m., caudal thigh) with 200 PFU ANDV diluted in 0.2 mL sterile PBS delivered with a 1mL syringe with a 25-gauge five-eighths-inch needle. All work involving hamsters were performed in an animal biosafety level 4 (ABSL-4) facility. Euthanasia was performed on hamsters meeting early endpoint criteria.

Research was conducted in compliance with the Animal Welfare Act and other federal statutes and regulations relating to animals and experiments involving animals and adheres to principles state in the Guide for the Care and Use of Laboratory Animals, National Research Council, 2011. The facilities where this research was conducted are fully accredited by the Association for Assessment and Accreditation of Laboratory Animal Care International.

N-specific ELISA assay:

ELISA plates (Costar, United States) were coated with recombinant PUUV N-antigen in carbonate buffer (pH 9.6) overnight at 4°C. Plates were blocked with PBS, 5% skim milk, and 0.05% Tween 20 (blocking solution) for 1 hour at 37°C, washed once with PBS and 0.05% Tween 20 (wash solution), and incubated with hamster sera diluted in blocking solution plus 2% *Escherichia coli* lysate for 30 minutes at 37°C. Plates were washed 3 times with wash buffer and incubated for 30 minutes at 37°C with horseradish peroxidase-conjugated goat anti-hamster IgG (Kikegaard & Perry Laboratories [KPL], USA) in blocking solution. Plates were washed 3 times with wash buffer and incubated for 10 minutes at room temperature with tetra-methylbenzidine substrate (KPL). The colorimetric reaction was stopped by adding Stop solution (KPL) and the absorbance at 450 nm was determined. The specific sum optical density (OD) was calculated by adding the background subtracted OD values, for dilutions whose OD was greater than the mean OD for serum samples from negative-control wells plus 3 standard deviations. The PUUV N antigen was used to detect not only PUUV but also ANDV N-specific antibody responses as previously reported (12). Hamster sera were heat inactivated before testing by ELISA.

Statistics

Data are expressed as mean values ± standard error of the mean. Statistical analysis was performed using 2-tailed Student t test. $P \leq 0.05$ was considered to be statistically significant. GraphPad Prism 6 software was used for the analysis.

RESULTS

Susceptibility of hantavirus towards gastric juice.

PUUV survival in the gastric lumen was tested *in vitro* by incubation of virus stocks to human gastric juice of varying pHs. The antiviral activity of gastric juice was effective at low pH between 1 and 3, with no virus surviving an exposure of as little as 1 minute. PUUV did survive exposure at pH values of 4 or 5 with an effective titer reduction below 1 $\log_{10}$ at pH 7 (Figure 1A).

Virus replication in Caco-2 monolayers

Prior to beginning experiments we confirmed that Caco-2 cells expressed ß1- and ß3-integrins as well as CD55/DAF, the receptors preferentially used by hantaviruses for entry, on their surface (data not shown). Experimental infection of human intestinal cells, Caco-2, with PUUV at MOI 0.1 revealed a time-dependent increase of intra- and extracellular viral load by quantitative RT-PCR assays (Figure 1B). The intracellular localization of hantavirus in Caco-2 cells could also be visualized by CLSM between 24 and 96 h post infection (p.i.). Hantavirus antigens were found intracellularly in co-localization with early endosomal antigen 1 (EEA1), demonstrating endosomal localization of virus particles (Figure 1C). In cells infected with UV-inactivated virus such signals were not present (data not shown).

Translocation of PUUV through Caco-2 monolayers after apical infection could be shown by qRT-PCR detection of viral RNA in basal culture medium. The basal release of viruses was detectable after 24 h and it increased by 2 $\log_{10}$ over the next 216 h (Figure 1D).

Epithelial barrier dysfunction in infected Caco-2 monolayers

Infection of Caco-2 monolayers at MOI 0.1 revealed stable TER values up to 48 h p.i., however, by 72 h p.i. the TER decreased to 60% of the initial value (Figure 2A). Using CLSM, viral antigen was observed intracellularly, in close proximity to the tight junctions, which exhibit condensed zonula occludens protein-1 (ZO-1) (Figure 2B). However, clear co-localization of PUUV and ZO-1, as evidenced by a lack of yellow signal, did not occur,

excluding a direct interaction. Moreover, the ZO-1 staining pattern could indicate a disturbed gate function (Figure 2C), by actomoysin-constriction mediated tight junction re-distribution, which could also lead to a loss of cell-cell contacts. To exclude the possible induction of cell death by apoptosis Caco-2 monolayers were stained by TUNEL 240 h p.i. Apoptotic events counted in PUUV-infected monolayers did not differ significantly from mock-infected monolayers (0.46% ± 0.10% versus 0.42% ± 0.05%, n=5, P = 0.73).

Infection of Caco-2 monolayers with higher concentrations of PUUV (MOI 1.0) revealed earlier and more pronounced effects (Figure 2C). Here, the condensation of ZO-1 was found by 48 h p.i., followed by disappearance of ZO-1 signals, and finally cell detachment and/or cell exfoliation leading to epithelial leakage by 96 h p.i.

Administration of PUUV intragastrically leads to productive infection in Syrian Hamsters

Groups of eight hamsters were instilled intragastrically with either 1,000 PFU PUUV or 10,000 PFU PUUV. To confirm that seroconversion was caused by active viral replication, and not input virus, a control group of eight hamsters was injected with 10,000 PFU γ-irradiated PUUV. 35 days post challenge the hamsters were bled, and seroconversion evaluated by N-ELISA (Figure 2D). 2/8 hamsters in the 1,000 PFU challenge group, and 3/8 hamsters in the 10,000 PFU challenge group seroconverted. None of the hamsters instilled with irradiated virus seroconverted, confirming that viral replication occurred in seroconverted animals.

Prior infection with PUUV is able to protect animals from lethal ANDV challenge. To confirm that hamsters which had seroconverted were truly infected, at 42 days post PUUV challenge all hamsters were challenged with 200 PFU of ANDV. 5/5 (100%) of the seroconverted hamsters survived ANDV challenge, confirming infection, while 15/19 (79%)

of non-seroconverted hamsters succumbed (n=24, P=0.003 according to Fisher´s exact test). The survival curves for PUUV intragastrically "vaccinated" hamsters are in Figure 2E.

DISCUSSION

Stomach physiology, survival in the gastric lumen

In the human alimentary tract entering viruses encounter gastric acid and proteolytic enzymes with gastric contents falling below pH 4 a maximum 70% of the time (15). pH values in human stomach can postprandially easily increase above pH 5.0, even, up to pH 7.0 in young children after consumption of food with high buffer capacity such as milk or milk products (15, 16). Stomach transit times can vary between 5 minutes and 2 hours, depending on food and liquid intake (17). Dyspepsia, which is diagnosed in up to 25% of western population, is treated with proton pump inhibitors (PPIs), leading to elevated pH and higher susceptibility to gastrointestinal infections (18).

In our study PUUV was shown to be able to survive human gastric juice for at least 15 min at pH 4, though viral titers were reduced by 3 $\log_{10}$. Exposed to gastric juice at pH 5 for 15 minutes, the reduction of virus titer amounted to 2 $\log_{10}$, and at pH 7 less than a 1 $\log_{10}$ loss of viability was observed, suggesting the virus can survive long enough to be viably released into the duodenum. Postprandial decreases in gastric pH can lead to reduced activity of gastric proteolytic enzymes, like pepsin A or pepsin C, making the environment even more conducive to viral survival. Under postprandial or achlorhydric conditions the antimicrobial gastric barrier is vulnerable and can be overcome by pathogens (15, 19). Finally, stomach conditions are dependent on the host's age, health status (gastric secretion rate), and nutritional preferences (buffer capacity of the food) leading to variable risk factors for hantavirus survival and therefore infection through the gastrointestinal tract.

Intragastric inoculation followed by a systemic infection has been previously demonstrated in the hamster model of hantavirus pulmonary syndrome using Andes virus (9). The intragastric 50% lethal dose (LD_{50}) of 225 plaque forming units (pfu), higher than the LD_{50} for both intranasal (LD_{50} = 95 pfu) and intramuscular (LD_{50} = 8 pfu) infection, indicating the route of infection was the least efficient of the three (9). The fact that the intragastric route leads to productive infection at all, however, suggests that it is a possible route of human infection. Moreover, the high pH of the rodent stomach (median of pH 3.1 - 4.5 in the mouse) in comparison to pH values known from humans (20) implicates an even easier transmission among the host animals.

Endocytotic cell entry

The small intestinal tissue, with its major resorptive function, is an entry site for pathogens including Norovirus or *Yersinia enterocolitica*. The MALT (mucosa-associated lymphoid tissue) is the site for replication and dissemination for several pathogens including HIV (21). In our experiments Caco-2-derived human intestinal epithelial cells are capable of being infected by PUUV. The virus localized to the endocytic pathway, as visualized by co-localization of virus N-protein with EEA1, as already shown for Hantaan virus in Vero-E6 cells (7), while the membrane ruffling visible at late time points of infection could be an additional sign of high endocytic activity. Moreover, interactions of pathogenic viruses with tight junction proteins containing PDZ domains (PSD-95/Dlg/ZO-1) or CAR (Coxsackie virus and adenovirus-receptor) have been frequently described (reviewed in 22) as have interactions between old world hantaviruses and DAF/CD55 (5). The data presented here, including the proximity of viral nucleocapsid protein to tight junctions together with ZO-1 ruffling, reinforce the idea that PUUV uses similar mechanisms during its infection of intestinal epithelial cells.

Epithelial barrier dysfunction

As the result of hantavirus infection, transcytotic viral uptake occurs as seen in our cell culture infection model, even at low MOIs. In cell culture experiments using higher viral concentrations, cell detachment and severe epithelial damage takes place with preceding cytoskeletal rearrangements (data not shown) and tight junction impairment. Finally, cell rounding and detachment lead to significant barrier dysfunction. Loss of cells due to apoptosis could be excluded, but cell exfoliation or shedding, as well as other cell death mechanisms like autophagy or necrosis, could play a role in the pathogenic action of hantaviruses in the gut. The latter condition may more accurately resemble clinical cases of hemorrhagic fever, where a manifestation of hantavirus disease is compromised endothelial barrier function leading to petechiae or even hemorrhages (2). Since disturbance of epithelial barrier function in the intestine leads to paracellular antigen influx (leaky gut concept [14]), entry of further virus particles and luminal bacterial antigens is possible. This could provoke immune activation and gastrointestinal symptoms like diarrhea, vomiting or abdominal pain, which are often found in clinical HFRS cases.

In the Syrian hamster model of intragastric PUUV infection we were able to confirm that the virus is capable of infecting, and replicating within the animal at a challenge dose of 1,000 PFU, as measured by seroconversion and protection from lethal ANDV challenge. Given the limited number of doses tested it is not possible to determine a precise infectious dose that infects 99% (ID99) of hamsters, however, given that only 3/8 hamsters infected with 10,000 PFU PUUV seroconverted the ID99 must be higher than that dose. This would make the ID99 for intragastric infection at least 10 fold higher than for intramuscular or intranasal (unpublished data, Hooper lab), indicating that while intragastric infection is possible; it is less efficient than other methods used in the laboratory.

Hantavirus route of infection

Here, we present evidence that the oral route of transmission, potentially by contaminated food, is plausible for PUUV. Furthermore, it is supposable that encapsulated virus particles from bronchioalveolar exudate can infect the host via the alimentary tract when swallowed, which is a common event. The results of our work denote a new aspect of hantavirus pathogenesis to be included in epidemiological considerations.

Acknowledgements. We are grateful to Brita Auste, Christine Spingies, and Britta Jebautzke for excellent technical assistance, as well as to Walid Azab and Annett Petrich for their methodical support. Opinions, interpretations, conclusions, and recommendations are those of the authors and not necessarily endorsed by the U.S. Army or the Department of Defense.

Financial support. This work was supported by the German Research Council (grants KR1293/13 to DHK and SCHU559/11 to JDS) and the German Federal Ministry for Education and Research in frame of Infect-ERA (grant 031L0096B to DHK). Work at USAMRIID was funded by the U.S. Army Medical Research and Material Command, Military Infectious Disease Research Program, Program Area T.

Potential conflicts of interest. All authors: No reported conflicts.

REFERENCES

1. Kruger DH, Figueiredo LT, Song JW, Klempa B. 2015. Hantaviruses--globally emerging pathogens. J Clin Virol 64:128-36.

2. Vaheri A, Strandin T, Hepojoki J, Sironen T, Henttonen H, Mäkelä S, Mustonen J. 2013. Uncovering the mysteries of hantavirus infections. Nat Rev Microbiol. 11(8):539-50.

3. Gavrilovskaya IN, Brown EJ, Ginsberg MH, Mackow ER. 1999. Cellular entry of hantaviruses which cause hemorrhagic fever with renal syndrome is mediated by beta3 integrins. J Virol 73(5):3951-9.

4. Raftery MJ, Lalwani P, Krautkrämer E, Peters T, Scharffetter-Kochanek K, Krüger R, Hofmann J, Seeger K, Krüger DH, Schönrich G. 2014. β2 integrin mediates hantavirus-induced release of neutrophil extracellular traps. J Exp Med. 211(7):1485-97.

5. Krautkrämer E, Zeier M. 2008. Hantavirus causing hemorrhagic fever with renal syndrome enters from the apical surface and requires decay-accelerating factor (DAF/CD55). J Virol 82(9):4257-64.

6. Krautkrämer E, Lehmann MJ, Bollinger V, Zeier M. 2012. Polar release of pathogenic Old World hantaviruses from renal tubular epithelial cells. Virol J 9:299.

7. Jin M, Park J, Lee S, Park B, Shin J, Song KJ, Ahn TI, Hwang SY, Ahn BY, Ahn K. 2002. Hantaan virus enters cells by clathrin-dependent receptor-mediated endocytosis. Virology 294(1):60-9.

8. Nuutinen H, Vuoristo M, Färkkilä M, Kahri A, Seppälä K, Valtonen V, Joutsiniemi T, Miettinen T. 1992. Hemorrhagic gastropathy in epidemic nephropathy. Gastrointest Endosc 38(4):476-80.

9. Hooper JW, Ferro AM, Wahl-Jensen V. 2008. Immune serum produced by DNA vaccination protects hamsters against lethal respiratory challenge with Andes virus. J Virol 82(3):1332-8.

10. Ruo SL, Li YL, Tong Z, Ma QR, Liu ZL, Tang YW, Ye KL, McCormick JB, Fisher-Hoch SP, Xu ZY. 1994. Retrospective and prospective studies of hemorrhagic fever with renal syndrome in rural China. J Infect Dis. 170(3):527-34.

11. Heider H, Ziaja B, Priemer C, Lundkvist A, Neyts J, Krüger DH, Ulrich R. 2001. A chemiluminescence detection method of hantaviral antigens in neutralization assays and inhibitor studies. J Virol Methods. 96(1):17-23.

12. Hooper JW, Larsen T, Custer DM, Schmaljohn CS. 2001. A lethal disease model for hantavirus pulmonary syndrome. Virology 289(1), 6-14.
13. Kramski M, Meisel H, Klempa B, Kruger DH, Pauli G, Nitsche A. 2007. Detection and typing of human pathogenic hantaviruses by real-time reverse transcription-PCR and pyrosequencing. Clin Chem 53(11):1899-905.
14. Bücker R, Schulz E, Günzel D, Bojarski C, Lee IF, John LJ, Wiegand S, Janßen T, Wieler LH, Dobrindt U, Beutin L, Ewers C, Fromm M, Siegmund B, Troeger H, Schulzke JD. 2014. α-Haemolysin of Escherichia coli in IBD: a potentiator of inflammatory activity in the colon. Gut 63(12):1893-1901.
15. Mitchell DJ, McClure BG, Tubman TR. 2001. Simultaneous monitoring of gastric and oesophageal pH reveals limitations of conventional oesophageal pH monitoring in milk fed infants. Arch Dis Child 84(3):273-6.
16. Bücker R, Azevedo-Vethacke M, Groll C, Garten D, Josenhans C, Suerbaum S, Schreiber S. 2012. Helicobacter pylori colonization critically depends on postprandial gastric conditions. Sci Rep 2:994.
17. Worsøe J, Fynne L, Gregersen T, Schlageter V, Christensen LA, Dahlerup JF, Rijkhoff NJ, Laurberg S, Krogh K. 2011. Gastric transit and small intestinal transit time and motility assessed by a magnet tracking system. BMC Gastroenterol 11:145.
18. Cook GC. 1994. Hypochlorhydria and vulnerability to intestinal infection. Eur J Gastroenterol Hepatol. 6(8):693-696.
19. Haastrup P, Paulsen MS, Begtrup LM, Hansen JM, Jarbøl DE. 2014. Strategies for discontinuation of proton pump inhibitors: a systematic review. Fam Pract 31(6):625-30.
20. Kararli TT. 1995. Comparison of the gastrointestinal anatomy, physiology, and biochemistry of humans and commonly used laboratory animals. Biopharm Drug Dispos 16(5):351-80.
21. Epple HJ, Allers K, Tröger H, Kühl A, Erben U, Fromm M, Zeitz M, Loddenkemper C, Schulzke JD, Schneider T. 2010. Acute HIV infection induces mucosal infiltration with CD4+ and CD8+ T cells, epithelial apoptosis, and a mucosal barrier defect. Gastroenterology 139(4):1289-300.

401 22. Zihni C, Balda MS, Matter K. 2014. Signalling at tight junctions during epithelial
402 differentiation and microbial pathogenesis. J Cell Sci 127(16):3401-13.

403

FIGURE LEGENDS

Figure 1. Infection of intestinal cells by hantavirus

A) Hantavirus survival in gastric juice. Infectious dose of 10^6 Puumala virus (PUUV) particles was suspended to pure gastric juice set to pH 1 - 7 with NaOH for 1, 10, or 15 min. After given incubation intervals the gastric juice was neutralized with NaOH and the virus suspension was used to infect VERO-E6 cells for focus titration of infectious particles. **B) Growth kinetics of hantaviruses in Caco-2 cells.** Caco-2 cells growing on cell culture slides were infected with PUUV at MOI of 0.1. Viral replication was monitored by qPCR in culture medium and cells. **C) Intracellular localization of hantavirus in Caco-2 cells.** Confocal laser-scanning microscopy (CLSM) of infected cell monolayers. Caco-2 cells growing on coverslips were infected with PUUV at MOI of 0.1. The cells were fixed with methanol-free formaldehyde and stained with antibodies against PUUV nucleocapsid protein (red) and early endosomal antigen 1 (EEA1, green). Cell nuclei were stained by DAPI (blue). **D) Translocation of hantavirus through polarized Caco-2 monolayers.** Caco-2 cells growing on filter inserts for at least 3 weeks were infected by PUUV at MOI 0.1. Apical and basal medium were collected at 24, 120, and 240 h p.i. and investigated for viral replication by qPCR.

Figure 2. Epithelial barrier dysfunction and loss of cellular integrity

A) Epithelial barrier dysfunction in infected Caco-2 monolayers. Caco-2 cells growing on filter inserts were infected by PUUV at MOI 0.1. Transepithelial electrical resistance (TER) was measured during infection with chopstick electrodes. **B) Tight junction disturbance.** Caco-2 cells grown on filter inserts were infected with PUUV at MOI of 0.1 and analyzed by

CLSM. At 48h cells were fixed and stained for PUUV nucleocapsid protein (red) and zonula occludens protein 1 (green). Cell nuclei were stained by DAPI (blue). **C) Leaks in Caco-2 cells monolayers at high MOI.** Caco-2 cells grown on coverslips were infected with PUUV at MOI of 1.0. At different time points the cells were fixed and stained with antibodies against PUUV nucleocapsid protein (red) and zonula occludens protein 1 (green) and analyzed by CLSM. Mock control is shown at 96 h. **D) Intragastral infection of hamster by Puumala virus.** Syrian hamsters (animal numbers given on the x-axis) were infected with either 1,000 PFU, 10,000 PFU or 10,000 PFU γ-irradiated PUUV. Thirty five days post infection hamsters were bled to test for seroconversion by N-ELISA. Dots represent hamsters for which subsequent ANDV challenge was lethal. **E) Survival curves for hamsters "vaccinated" intragastrically with PUUV.** 42 days post intragastric PUUV challenge, the same hamsters were challenged with 200 PFU ANDV i.m.

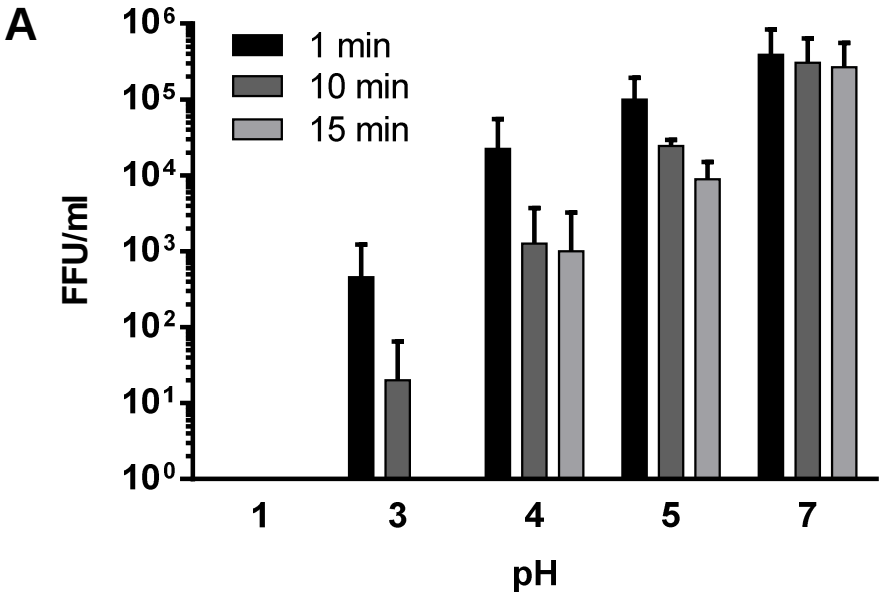
A
FFU/ml
1 min
10 min
15 min
pH
1
3
4
5
7

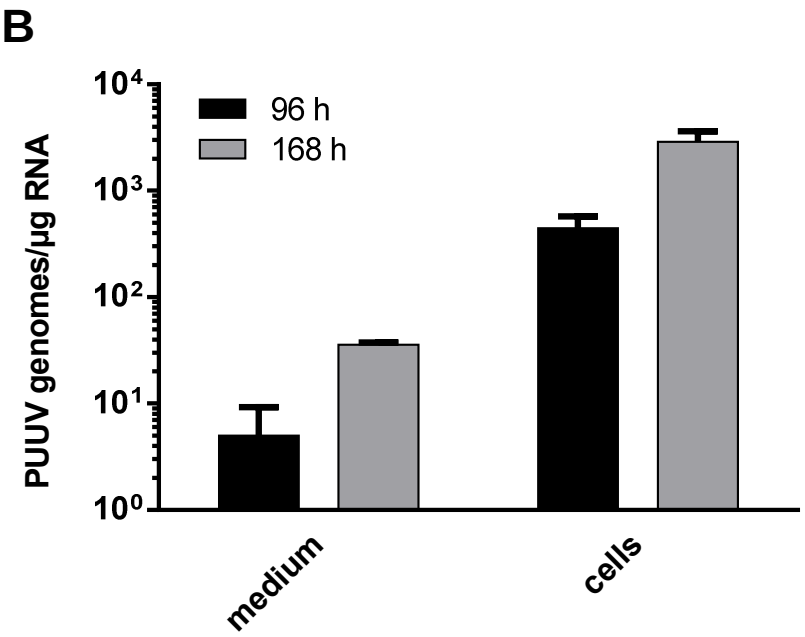
B
PUUV genomes/µg RNA
96 h
168 h
medium
cells

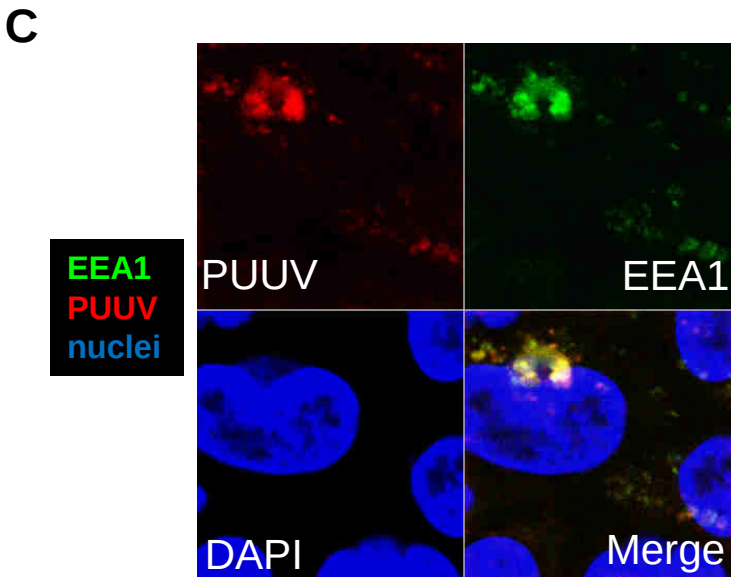
C
EEA1
PUUV
nuclei
PUUV
EEA1
DAPI
Merge

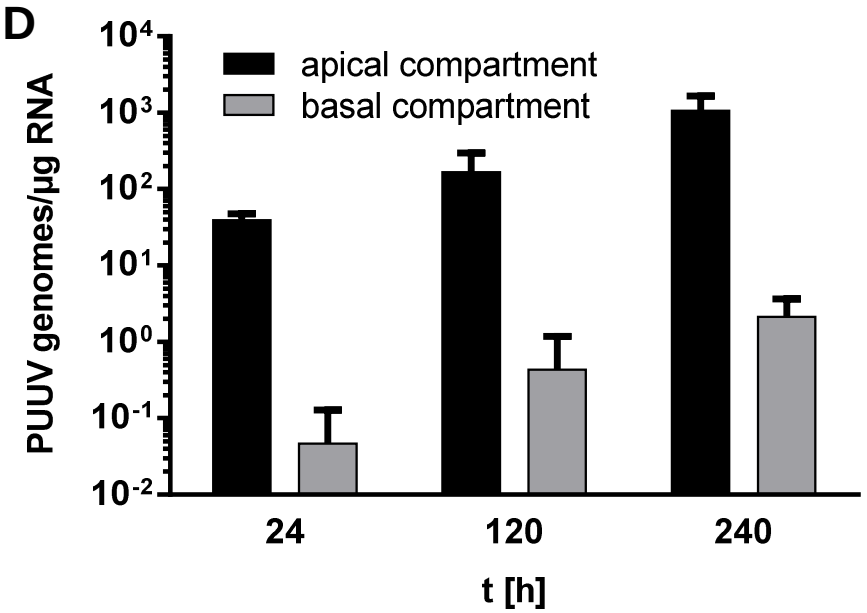
D
PUUV genomes/µg RNA
apical compartment
basal compartment
24
120
240
t [h]

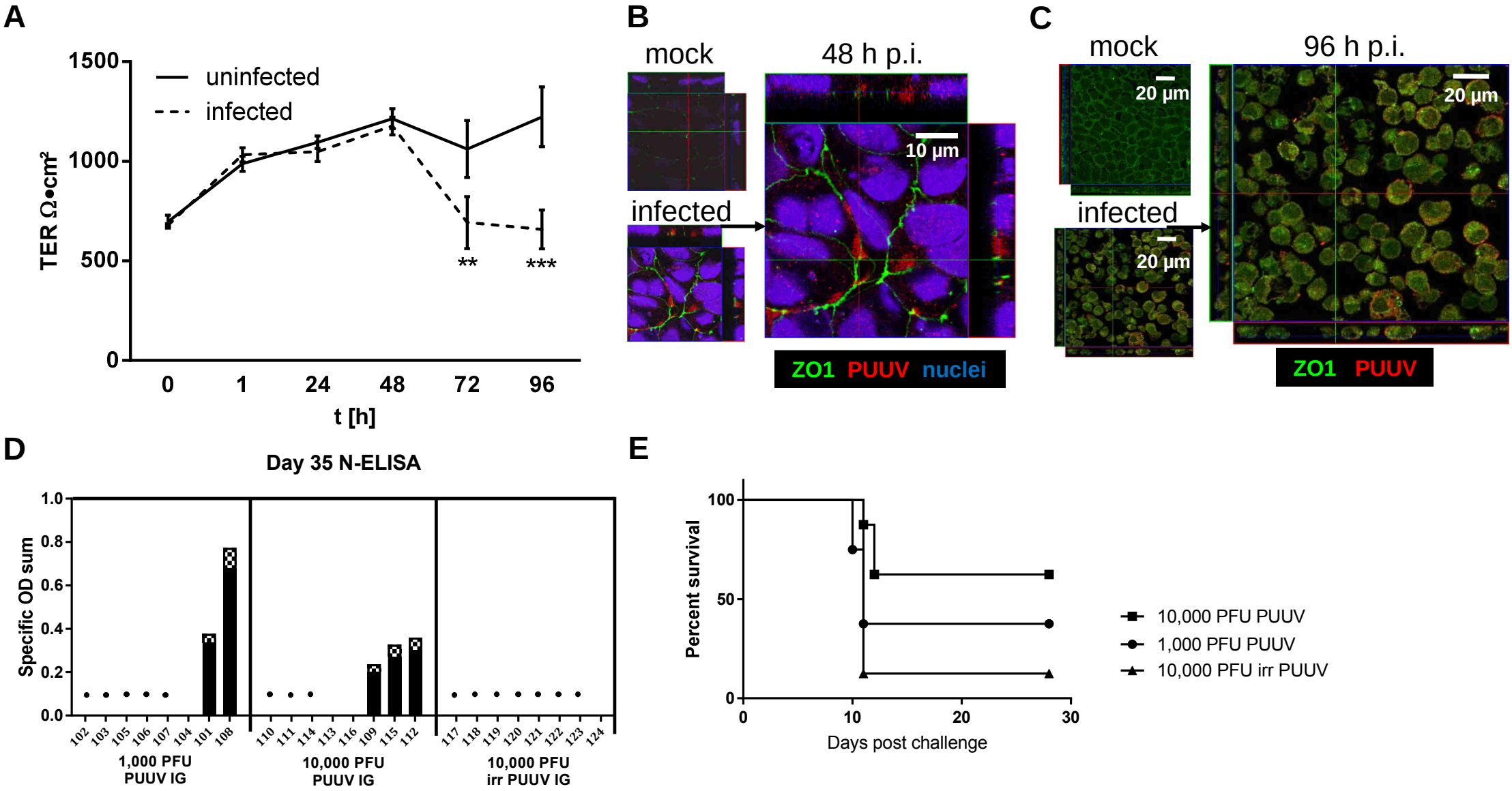
A
1500
1000
500
0
TER Ω•cm²
uninfected
infected
**
***
0
1
24
48
72
96
t [h]
B
mock
48 h p.i.
infected
10 µm
ZO1 PUUV nuclei
C
mock
96 h p.i.
20 µm
20 µm
infected
20 µm
ZO1 PUUV
D
Day 35 N-ELISA
Specific OD sum
1.0
0.8
0.6
0.4
0.2
0.0
102 103 105 106 107 104 101 108
1,000 PFU PUUV IG
110 111 114 113 116 109 115 112
10,000 PFU PUUV IG
117 118 119 120 121 122 123 124
10,000 PFU irr PUUV IG
E
Percent survival
100
50
0
0
10
20
30
Days post challenge
10,000 PFU PUUV
1,000 PFU PUUV
10,000 PFU irr PUUV